

Aluminum–Ligand Cooperative N–H Bond Activation and an Example of Dehydrogenative Coupling

Thomas W. Myers and Louise A. Berben*

Department of Chemistry, University of California, Davis, California 95616, United States

Supporting Information

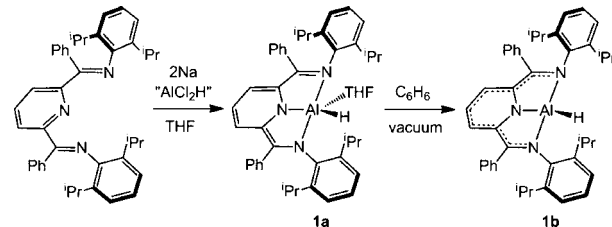
ABSTRACT: Activation of N–H bonds by a molecular aluminum complex via metal–ligand cooperation is described. ($^{Ph}I_2P^{2-}$)AlH (**1b**), in which $^{Ph}I_2P^{2-}$ is a tridentate bis(imino)pyridine ligand, reacts with anilines to give the N–H-activated products ($^{Ph}HI_2P^-$)AlH–(NHA_r) (**2**). When heated, **2** releases H₂ and affords ($^{Ph}I_2P^-$)Al(NHA_r) (**3**). Complex **1b** catalyzes the dehydrogenative coupling of benzylamine to afford H₂, NH₃, and *N*-(phenylmethylene)benzenemethanamine.

To develop sustainable catalytic transformations using abundant metals such as aluminum, an understanding of bond activation reactions is a necessary first step. Introducing functionality into unactivated bonds continues to be of significant interest, and in particular, the activation of N–H bonds often relies on the oxidative addition of N–H bonds to a transition-metal center.¹ However, the activation of N–H bonds via oxidative addition to transition metals can be impeded by the tendency of the Lewis basic nitrogen atom to bind open coordination sites.² In contrast, heterolytic activation of N–H bonds is more likely to remain feasible even when amine coordination occurs as a first step.²

A heterolytic reaction pathway has led to limited but fruitful examples of N–H activation in both transition-metal and main-group chemistry. Milstein and co-workers reported the heterolytic activation of amines by Ru pincer complexes via a metal–ligand cooperative pathway.³ Subsequently the complexes were shown to effect catalytic amine dehydrogenation.⁴ Heterolytic activation of N–H bonds has also been accomplished via main-group frustrated Lewis pairs to achieve catalytic hydrogenation of unsaturated systems.⁵ To date, main-group-mediated reactions have afforded stoichiometric N–H activation of aniline and ammonia⁶ and both stoichiometric and catalytic dehydrogenation of amine boranes.⁷ Heterolytic activation of alkynes has been observed at gallium.⁸

We previously explored the redox chemistry of iminopyridine complexes of aluminum.⁹ Herein we report aluminum complexes of a tridentate bis(imino)pyridine ligand that is henceforth denoted by $^{Ph}I_2P$ (see Scheme 1 for its structure). We isolated the tetrahydrofuran (THF)-adduct and base-free aluminum hydride complexes ($^{Ph}I_2P^{2-}$)AlH(THF) (**1a**) and ($^{Ph}I_2P^{2-}$)AlH (**1b**) and found that **1b** effects activation of the N–H bonds in anilines via a metal–ligand cooperative pathway. These reactions afford ($^{Ph}HI_2P^-$)AlH(NHA_r) [Ar = 2,6-diisopropylphenyl (Dipp) (**2a**), Ph (**2b**)]. When these complexes are heated, they release H₂, forming four-coordinate

Scheme 1



($^{Ph}I_2P^{2-}$)Al(NHA_r) [_r = Dipp (**3a**), Ph (**3b**)]. The syntheses of the aluminum hydride complexes followed a procedure adapted from our previous work on the related iminopyridine ligand system (Scheme 1).⁹ The $^{Ph}I_2P$ ligand and 2 equiv of sodium metal were stirred together in THF for 24 h, during which time the initial green solution became dark purple. After addition of an “ $AlCl_2H$ ” solution¹⁰ and subsequent workup, **1a** was isolated as a burgundy powder in 71% yield. Complex **1a** was found to be diamagnetic, and the proton NMR spectrum was informative (Figure S1 in the Supporting Information). A broad feature at 4.60 ppm corresponded to the Al–H proton, and the resonances for the THF ligand were observed as broad singlets at 3.59 and 1.37 ppm. The IR spectrum displayed an Al–H stretching band at 1966 cm⁻¹ (Figure S2 and Table S1), which is within the range for other known terminal aluminum hydride complexes.¹¹

Single crystals of **1a** were grown via slow diffusion of pentane into a concentrated THF solution of **1a**, and the structure was determined by single-crystal X-ray diffraction (Figure 1). The geometry at the Al center is very close to square-pyramidal,

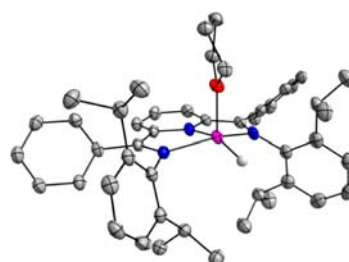


Figure 1. Solid-state structure of ($^{Ph}I_2P^{2-}$)AlH(THF) (**1a**). Pink, red, blue, gray, and white ellipsoids represent Al, O, N, C, and H atoms, respectively. The thermal ellipsoids have been set at 50% probability, and H atoms (except hydride) have been omitted.

Received: April 2, 2013

Published: June 25, 2013

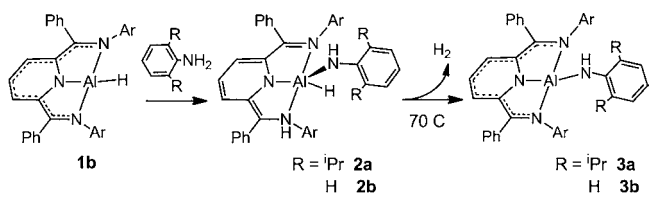


with $\tau = 0.117$.¹² The bond lengths in **1a** are consistent with a twice-reduced oxidation state of the ligand, where the two-electron reduction event is formally localized at the pyridine nitrogen and one of the imine nitrogens (Tables S2 and S3).^{9,13} Thus, the ligand is asymmetric with one formally imine N-donor [$\text{Al}-\text{N}_{\text{im}} = 2.077(2)$ Å], an anionic pyridine [$\text{Al}-\text{N}_{\text{py}} = 1.851(2)$ Å], and one anionic amido N-donor [$\text{Al}-\text{N}_{\text{am}} = 1.954(2)$ Å]. The C–C bond distances in the pyridine ring alternate between long [1.405(3) Å] and short [1.380(3) Å], consistent with a loss of aromaticity. These results are also in agreement with the diamagnetism observed by NMR spectroscopy.

Extraction of **1a** into benzene followed by evaporation of the solvent in vacuo led to removal of THF from the Al coordination sphere and the formation of the tan-colored four-coordinate complex **1b**, as identified by ^1H NMR spectroscopy. The ^1H NMR spectrum indicated that the oxidation state of the ligand remained unchanged at 2-, that the Al–hydride resonance had shifted downfield to 4.74 ppm, and that the THF ligand resonances were no longer apparent (Figure S3). The IR absorption band for Al–H also shifted by 185 cm⁻¹ to 1781 cm⁻¹ (Figure S2). We could not obtain single crystals of **1b**, but all of the data we did acquire, including the results of combustion analysis, were consistent with the assignment of **1b** as four-coordinate $(^{\text{Ph}}\text{I}_2\text{P}^{2-})\text{AlH}$. The electronic structure of the $^{\text{Ph}}\text{I}_2\text{P}^{2-}$ ligand, according to the ^1H NMR spectrum, is consistent with that of **3a** (*vide infra*). When **1b** was dissolved in THF, **1a** was observed in quantitative NMR yield.

Addition of H₂NDipp to a tan benzene solution of **1b** led to the immediate formation of a dark-blue solution (Scheme 2).

Scheme 2



X-ray diffraction analysis performed on a single crystal grown from the product revealed it to be $(^{\text{Ph}}\text{I}_2\text{P}^{2-})\text{AlH}(\text{NHDipp})$ (**2a**), in which the N–H bond of H₂NDipp was added across the aluminum–amido bond in **1b** (Figure 2 left). To probe whether **2a** might have been the result of the large steric

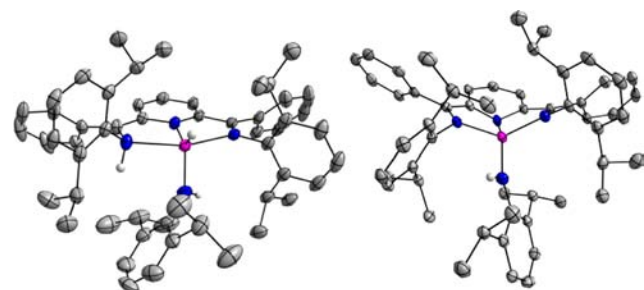


Figure 2. Solid-state structures of $(^{\text{Ph}}\text{I}_2\text{P}^{2-})\text{AlH}(\text{NHDipp})$ (**2a**) and $(^{\text{Ph}}\text{I}_2\text{P}^{2-})\text{Al}(\text{NHDipp})$ (**3a**). Pink, blue, gray, and white ellipsoids represent Al, N, C, and H atoms, respectively. The thermal ellipsoids have been set at 50% probability, and H atoms (except the hydride and N-bound protons) have been omitted.

demand of the NHDipp⁻ group, the reaction of **1b** with 1 equiv of aniline was investigated, and this led to formation of an analogous dark-blue product identified as $(^{\text{Ph}}\text{I}_2\text{P}^{2-})\text{AlH}(\text{NPh})$ (**2b**) by ^1H NMR spectroscopy. In both **2a** and **2b**, the amido nitrogen atom of $^{\text{Ph}}\text{I}_2\text{P}^{2-}$ is protonated and the resulting anilido ligand is coordinated to the Al center.

Complexes **2a** and **2b** were found to be diamagnetic, and their ^1H NMR spectra clearly showed that protonation of the amido nitrogen in $^{\text{Ph}}\text{I}_2\text{P}^{2-}$ induced a higher degree of asymmetry to the ligand than was observed in **1a** or **1b** (Figures S4 and S5). For instance, all of the protons on the pyridine ring became inequivalent. The single-crystal X-ray structures for **2a** and **2b** confirmed the higher degree of asymmetry of the protonated $^{\text{Ph}}\text{I}_2\text{P}^{2-}$ ligand in comparison with $^{\text{Ph}}\text{I}_2\text{P}^{2-}$ in **1a**. For example, the alternating single and double bonds in the dearomatized pyridine ring of $^{\text{Ph}}\text{I}_2\text{P}^{2-}$ were even more distinct than they were in **1a** (Tables S2 and S3).

When either **2a** or **2b** was heated at 70 °C for several hours in toluene, 1 equiv of H₂ was released, as measured by GC-TCD analysis. The formation of the corresponding new red-brown four-coordinate complexes $(^{\text{Ph}}\text{I}_2\text{P}^{2-})\text{Al}(\text{NAr})$ [Ar = Dipp (**3a**), Ph (**3b**)] was concomitantly observed. Both **3a** and **3b** are diamagnetic, and their proton NMR spectra were similar to that of four-coordinate **1b** (Figures S6 and S7). To probe the mechanism of formation of **2b** and its conversion to **3b**, aniline-^d₇ was employed. The ^1H NMR spectrum of **2b-d**₇ showed diminished intensity for the two N–H resonances and no change in the Al–H resonance (Figure S8). When **2b-d**₇ was heated, HD gas was observed (Figure S9), and the spectrum of **3b-d**₆ showed a decrease in the intensity of the N–H resonance (Figure S10). These results are in accord with Scheme 2.

Single crystals of **3a** were grown by chilling a concentrated hexane solution of **3a** at -25 °C for 3 days, and the X-ray crystal structure was determined (Figure 2 right). Complex **3a** is four-coordinate and best described as distorted tetrahedral, with a tetrahedrality of 51.6°.¹⁴ Notably, N_{py} no longer lies in plane with the rest of $^{\text{Ph}}\text{I}_2\text{P}^{2-}$: the N_{im}–C_{im}–C_{py(o)}–N_{py} torsion angles are 5.2° and 8.1°, as compared to 1.5° and 1.87° in **1a**. This deviation presumably stems from the preference of the Al center for a tetrahedral geometry, which conflicts with the preference of $^{\text{Ph}}\text{I}_2\text{P}^{2-}$ to be planar. The displacement of N_{py} from the plane removes it from the conjugated π system of the rest of the ligand, affording a symmetric conjugated system involving the N_{im}, C_{im}, and C_{py} atoms (Scheme 2 and Figure 2 right). The two C_{im}–N_{im} bond lengths are very similar at 1.374(3) and 1.370(3) Å, and this distance falls between that commonly observed for true C_{im}–N_{im} single and double bonds, as in the asymmetric closed-shell form of $^{\text{Ph}}\text{I}_2\text{P}^{2-}$. The two C_{im}–C_{py(o)} bond lengths are also very similar at 1.424(3) and 1.426(3) Å, and the C–C bonds in the pyridine ring [1.394(3), 1.397(3), 1.399(3), and 1.383(3) Å] are equivalent and longer than the bonds in neutral pyridine. The symmetry of this geometric structure suggests an electronic structure similar to the biradical triplet state commonly observed with bis(imino)pyridine ligands, in which a radical resides on each of the C_{im} atoms.¹³ However, the bond lengths and angles in **3a** are more consistent with a structure in which these radicals are somewhat delocalized and, as indicated by NMR spectroscopy, anti-ferromagnetically coupled. Antiferromagnetic coupling in a two-electron-reduced bis(imino)pyridine ligand was observed previously in a nickel(II) complex.¹⁵ Notably, in that case the

I_2P ligand was also distorted from planarity with $\text{N}_{\text{im}}-\text{C}_{\text{im}}-\text{C}_{\text{py}(\text{o})}-\text{N}_{\text{py}}$ torsion angles of 11.87° and 11.45° .

The ability of **1b** to activate N–H bonds via a metal–ligand cooperative mechanism prompted us to investigate its potential as an amine dehydrogenation catalyst. Benzylamine and 20 mol % **1b** was heated at reflux in toluene at 70°C for 24 h, and the formation of *N*-(phenylmethylene)benzenemethanamine was observed with 75% conversion and 3.6 turnovers, as measured by GC–MS (Figure S11).¹⁶ The formation of stoichiometric H_2 and NH_3 was observed by GC-TCD (Figure S12).

In conclusion, we have shown that a bis(imino)pyridine complex of aluminum activates N–H bonds via a metal–ligand cooperative mechanism and that this N–H bond activation event can initiate amine dehydrogenation catalysis and convert benzylamine into the homocoupled imine. Efforts to expand the scope of the bond activation and catalysis observed here are underway.

ASSOCIATED CONTENT

Supporting Information

Preparation of complexes; X-ray data for **1a**, **2a**, and **3a**; CIF files; IR and NMR spectra; and GC-TCD and GC–MS data. This material is available free of charge via the Internet at <http://pubs.acs.org>.

AUTHOR INFORMATION

Corresponding Author

laberben@ucdavis.edu

Notes

The authors declare no competing financial interest.

ACKNOWLEDGMENTS

We thank the Alfred P. Sloan Foundation for support of this work.

REFERENCES

- (1) (a) Farfar, C. M.; Adhikari, D.; Foxman, B. M.; Mindiola, D. J.; Ozerov, O. V. *J. Am. Chem. Soc.* **2007**, *129*, 10318. (b) Zhao, J.; Goldman, A. S.; Hartwig, J. F. *Science* **2005**, *307*, 1080. (c) Kanzelberger, M.; Zhang, X.; Emge, T. J.; Goldman, A. S.; Zhao, J.; Incarvito, C.; Hartwig, J. F. *J. Am. Chem. Soc.* **2003**, *125*, 13644. (d) Koelliker, R.; Milstein, D. *J. Am. Chem. Soc.* **1991**, *113*, 8524.
- (2) Sykes, A. C.; White, P.; Brookhart, M. *Organometallics* **2006**, *25*, 1664.
- (3) (a) Khaskin, E.; Iron, M. A.; Shimon, L. J. W.; Zhang, J.; Milstein, D. *J. Am. Chem. Soc.* **2010**, *132*, 8542. (b) Feller, M.; Diskin-Posner, Y.; Shimon, L. J. W.; Ben-Ari, E.; Milstein, D. *Organometallics* **2012**, *31*, 4083.
- (4) He, L. P.; Chen, T.; Gong, D.; Lai, Z.; Huang, K. W. *Organometallics* **2012**, *31*, 5208.
- (5) (a) Chase, P. A.; Welch, G. C.; Jurca, T.; Stephan, D. W. *Angew. Chem., Int. Ed.* **2007**, *46*, 8050. (b) Greb, L.; Oña-Burgos, P.; Schrimmer, B.; Grimme, S.; Stephan, D. W.; Paradies, J. *Angew. Chem., Int. Ed.* **2012**, *51*, 10164. (c) Mahdi, T.; Heiden, Z. M.; Grimme, S.; Stephan, D. W. *J. Am. Chem. Soc.* **2012**, *134*, 4088. (d) Chase, P. A.; Jurca, T.; Stephan, D. W. *Chem. Commun.* **2008**, *1701*. (e) Privalov, T. *Chem.—Eur. J.* **2009**, *15*, 1825.
- (6) (a) Jana, A.; Schulzke, C.; Roesky, H. W. *J. Am. Chem. Soc.* **2009**, *131*, 4600. (b) Chase, P. A.; Stephan, D. W. *Angew. Chem., Int. Ed.* **2008**, *47*, 7433.
- (7) (a) Miller, A. J. M.; Bercaw, J. E. *Chem. Commun.* **2010**, *46*, 1709. (b) Bellham, P.; Hill, M. S.; Kociok-Köhn, G.; Liptrot, D. J. *Chem. Commun.* **2013**, *49*, 1960. (c) Less, R. J.; Simmonds, H. R.; Dane, S. B. J.; Wright, D. S. *Dalton Trans.* **2013**, *42*, 6337. (d) Cowley, H. J.; Holt, M. S.; Melen, R. L.; Rawson, J. M.; Wright, D. S. *Chem. Commun.* **2011**, *47*, 2682.
- (8) (a) Fedushkin, I. L.; Khvojina, N. M.; Skatova, A. A.; Fukin, G. K. *Angew. Chem., Int. Ed.* **2003**, *42*, 5223. (b) Fedushkin, I. L.; Morozov, A. G.; Rassadin, O. V.; Fukin, G. K. *Chem.—Eur. J.* **2005**, *11*, 5749. (c) Fedushkin, I. L.; Skatova, A. A.; Fukin, G. K.; Hummert, M.; Schumann, H. *Eur. J. Inorg. Chem.* **2005**, 2332.
- (9) (a) Myers, T. W.; Kazem, N.; Stoll, S.; Britt, R. D.; Shanmugam, M.; Berben, L. A. *J. Am. Chem. Soc.* **2011**, *133*, 8662. (b) Myers, T. W.; Berben, L. A. *J. Am. Chem. Soc.* **2011**, *133*, 11865. (c) Myers, T. W.; Berben, L. A. *Inorg. Chem.* **2012**, *51*, 8997.
- (10) Formed in situ from $\text{LiAlH}_4 + 3\text{AlCl}_3$ in THF.
- (11) For example, see: (a) Kuo, P. C.; Chem, I. C.; Chang, J. C.; Lee, M. T.; Hu, C. H.; Hung, C. H.; Lee, H. M.; Huang, J. H. *Eur. J. Inorg. Chem.* **2004**, 4898. (b) Alexander, S. G.; Cole, M. L.; Forsyth, C. M.; Furfari, S. K.; Konstas, K. *Dalton Trans.* **2009**, 2326.
- (12) Addison, A. W.; Rao, T. N.; Van Rijn, J. J.; Verschoor, G. C. J. *Chem. Soc., Dalton Trans.* **1984**, 1349.
- (13) Bowman, A. C.; Milsmann, C.; Atienza, C. C. H.; Lobkovsky, E.; Wieghardt, K.; Chirik, P. J. *J. Am. Chem. Soc.* **2010**, *132*, 1676.
- (14) Battaglia, L. P.; Corradi, A. B.; Marcotrigiano, G.; Menabue, L.; Pellaiani, G. C. *Inorg. Chem.* **1979**, *18*, 148.
- (15) Ghosh, M.; Weyhermüller, T.; Wieghardt, K. *Dalton Trans.* **2010**, *39*, 1996.
- (16) This is comparable to turnover numbers achieved using main-group amine borane dehydrogenation catalysts.⁷